Prolific release of S-layer units and associated proteins by the methanotrophic bacterium *Methylomicrobium album* BG8

Running title: S-layer units released by *Methylomicrobium album* BG8

Mariah K. Hermary [a,*], Maria C. Rodriguez Gallo [a], Aurelija M. Grigonyte [b], R. Glen Uhrig [a], Dominic Sauvageau [b], and Lisa Y. Stein [a#]

[a]Department of Biological Sciences, University of Alberta, Edmonton AB Canada T6G 2E9

[b]Department of Chemical and Materials Engineering, University of Alberta, Edmonton AB Canada T6H 1H9

*Current Address: Alberta Agriculture and Irrigation, Government of Alberta, Edmonton AB T6H 4P2

#Corresponding Author: CW 405 Bio Sci Bldg, lisa.stein@ualberta.ca

Abstract. Some gammaproteobacterial methanotrophs are encapsulated by S-layers that overlay their outer membrane. In this study, TEM imaging revealed that *Methylomicrobium album* BG8 constitutively releases abundant cup-shaped S-layer units – a phenotype that was not observed in 7 other methanotroph strains, even in *Methylotuvimicrobium buryatense* 5GB1 that produces a similar S-layer structure. Release of S-layer units occurred regardless of carbon (methane or methanol) or nitrogen (ammonium or nitrate) source, with 50X trace metal availability or under copper deprivation, and at all growth phases. The released S-layer units were isolated from the culture medium of *M. album* BG8 for proteome analysis. The proteome revealed an abundance of transporters related to calcium uptake including TolC and Repeats-in-Toxin (RTX) proteins, transporters for uptake for cobalamin and siderophores, proteins with Type I secretion system (T1SS) target domains, cell wall biogenesis proteins, and the S-layer protein units themselves. The gene encoding the S-layer protein is co-located in the *M. album* BG8 genome with genes encoding the T1SS. Together, this information provides clues regarding *M. album* BG8 S-layer biogenesis and function, including a role for the calcium and RTX protein domains, involvement of the T1SS in selecting associated proteins, and reasons behind prolific release of S-layer units. This S-layer release and involvement of the T1SS has biological implications and could be applied towards selective secretion of proteins by *M. album* BG8 in bioindustrial applications.

Importance. The methanotrophic bacterium *M. album* BG8 produces and releases large quantities of its S-layer units into the culture medium regardless of carbon or nitrogen source, metal availability or phase of growth. Of the 8 methanotrophic bacteria screened, only *M. album* BG8 possesses this phenotype. Proteomics analysis of purified S-

layer units identified the S-layer protein itself along with associated proteins involved metal uptake and S-layer biogenesis, including involvement of the T1SS. Better understanding of *M. album* BG8 S-layer biogenesis and the release of its S-layer units into culture medium could be harnessed for exporting expressed proteins of bioindustrial interest for ease of collection and purification.

Introduction

Aerobic methanotrophic bacteria are clustered within the Gammaproteobacteria, Alphaproteobacteria and Verrucomicrobia phyla and are metabolically differentiated by their discrete pathways of carbon assimilation (1). Collectively, methanotrophs are of industrial interest for their capacity to convert methane, a potent greenhouse gas, into valuable molecules, from biopolymers to proteins to biofuels (2). The gammaproteobacterium *Methylomicrobium album* BG8 is a high priority strain for industrialization due to its metabolic flexibility to grow rapidly on methane or methanol as a carbon source and with nitrate or ammonium as a nitrogen source (3, 4) and availability of its genome-scale metabolic model (5).

Structural analysis of methanotroph cell surfaces has revealed that some halophilic strains possess unique S-layers comprised of tightly packed cup-shaped protein units with p6 hexagonal symmetry (6-9). It was hypothesized that these structures could provide rigidity to the cell wall and play a role in osmoregulation and tolerance to extremes of salinity and alkalinity (9). However, non-halotolerant and neutralophilic methanotrophs, such as *Methylomicrobium album* BG8 (10) and *Methylomicrobium* sp. HG-1 (11), have similar arrays of these cup-like structures on their surfaces, which brings the physiological

63 role and mechanism of biogenesis of these S-layer structures into question. The copper-
64 repressible CorA protein has been indicated as the anchoring point of the cup-shaped S-
65 layer protein units onto the cell surface of *Methylotuvimicrobium alkaliphilum* 20Z (8). In *M.*
66 *album* BG8, isolated CorA protein was shown to bind copper (12) and, in mutants of both *M.*
67 *album* BG8 (13) and *M. alkaliphilum* 20Z, loss of CorA function resulted in a poor growth
68 phenotype on methane (8), but not on methanol. Thus, CorA likely plays a dual role in both
69 copper acquisition and S-layer protein attachment and facilitates methane oxidation
70 capability. *Caulobacter crescentus* also forms S-layers from cup-shaped RsaA proteins with
71 p6 symmetry (14). These RsaA proteins are secreted through a Type I secretion system
72 (T1SS) and contain a span of six repeat-in-toxin (RTX) domains that bind calcium to
73 promote folding and stabilization of the crystalline S-layer lattice (15).
74 The present study shows that *M. album* BG8 constitutively releases its cup-shaped S-
75 layer units under a variety of media. The cup-shaped S-layer units were purified from
76 culture medium, and proteomic analysis by LC-MS/MS was performed. Together, the
77 observations from this study provide understanding of the morphology, biogenesis, and
78 associated protein functions for released S-layer units of *M. album* BG8, including
79 involvement of the T1SS and calcium binding. Insights into the biogenesis of S-layer protein
80 units and their prolific release from the cell can be used as tools in the production and
81 secretion of valuable industrial proteins using single-carbon molecules as feedstocks.
82

83 **Results**

84 ***M. album* BG8 constitutively releases abundant cup-shaped S-layer units.**
85 Transmission electron microscopy of *M. album* BG8 displayed cup-shaped particles with

86 diameters ranging from 49.5 to 75.2 nm with an average of 60.9 ± 5.7 nm (n=50; Table 1).
87 Released S-layer units were observed when *M. album* BG8 was grown in NMS or AMS media
88 containing methane or methanol as a sole carbon source, media devoid of copper, and
89 media containing 50X trace elements solution (Fig. 1). Thus, release of S-layer protein units
90 was considered constitutive, as it did not vary with changes in carbon source, nitrogen
91 source, or metal availability. Released S-layer protein units were also present immediately
92 after culture inoculation, in mid-log growth and at stationary phase (images not shown).
93 However, released S-layer protein units were not detected in the medium of 7 other
94 methanotrophic strains examined (Fig. 2), including cultures of *Methylotuvimicrobium*
95 *buryatense* 5GB1, which possess similar cup-shaped S-layer lattices on its cell surface (9).
96 **S-layer unit proteome suggests associated functions of T1SS, calcium uptake,**
97 **metal acquisition, and membrane assembly.** From the total of 310 peptides identified by
98 LC-MS/MS from purified S-layer units released into the medium of *M. album* BG8 cultures
99 (Supplemental Table 1), 14 had high statistical significance across triplicate samples
100 (ranking PSM >4, peptides >5, and score>20). Of note were the S-layer protein itself
101 (H8GFV3), proteins related to binding and uptake of calcium and S-layer assembly (Ca^2 -
102 binding RTX protein, PtrC metalloprotease, pre-pilin N-terminal cleavage) (15-17),
103 proteins for siderophore and divalent cation uptake (TonB receptor) and cobalamin
104 transport (OM receptor), a protein with a T1SS C-terminal target domain, and a LPS-
105 assembly protein (Fig. 3, Table 2). Homologues to these and the other significantly
106 abundant proteins were searched for in the genomes of the four gammaproteobacterial
107 methanotrophs screened in this study, and only *Methylomonas denitrificans* FJG1 and *M.*
108 *buryatense* 5GB1 were found to encode a complete set of T1SS proteins with high

109 percentage identities to those found in *M. album* BG8 (Fig. 3). On the other hand, while *M.*
110 *denitrificans* FJG1 does not encode a homologue to the S-layer protein and did not have a
111 visible S-layer (Fig. 2), *M. buryatense* 5GB1 does encode an S-layer protein homologue with
112 33% amino acid identity (Fig. 3) and produces similar S-layers to *M. album* BG8 on its
113 surface (9), even though they were not visible by our TEM analysis (Fig. 2).

114 Proteins with relevance to S-layer biogenesis, but with lower statistical significance
115 (PSM $\leq$5, peptides $\leq$5, score $\leq$20), include TolC, which is the outer-membrane channel
116 component of the T1SS that interacts with the Ca^{2+} binding domains of RTX proteins for
117 their secretion (Table 3) (18). Several membrane-related proteins with lower statistical
118 significance included a cation diffusion facilitator protein, a general secretion pathway
119 "protein D", and TolB from the Tol-Pal system that may have been surreptitiously attached
120 to the released S-layer proteins units. OmpA protein, also associated with the S-layer
121 proteins, may play a role in S-layer biogenesis or tethering to the cell wall as it is an
122 abundant and vital protein in Gram negative bacteria (19). CorA, the protein thought to
123 anchor S-layer proteins to the cell wall (8), was only found in one of the triplicate proteome
124 samples at low abundance. Abundant flagella-related proteins were co-purified, likely as
125 contaminants from the culture supernatant.

126

127 **Discussion**

128 Based on the most abundant proteins with annotated functions in the proteome of
129 released *M. album* BG8 S-layer units, we can surmise that their biogenesis occurs through
130 calcium-mediated secretion of S-layer proteins via the Ca^{2+}-binding RTX domains of the
131 T1SS (17, 18) and are assembled with assistance of several outer membrane and other

132 RTX-domain proteins (16, 17). The T1SS has three components: an ABC transporter located
133 within the inner membrane, a membrane fusion protein that spans the periplasmic space,
134 and an outer membrane porin protein to create an ATP-dependent translocation
135 mechanism (18). TolC, an abundant protein in the *M. album* BG8 S-layer unit proteome,
136 forms the outer membrane porin component of the T1SS and transports Ca^{2+}-binding
137 proteins via a Ca^{2+} ratcheting mechanism (18). The protein targets of the T1SS are typically
138 defined by several blocks of nonapeptide-binding consensus sequences located at their C-
139 termini (20). The identification of significant RTX exoprotein and T1SS C-terminal target
140 domain protein in the S-layer unit proteome suggests these T1SS secreted proteins are also
141 associated with the S-layer structure. The significant abundance of associated PrtC
142 metalloprotease suggests a putative role in S-layer biogenesis, or maintenance, analogous
143 to what is observed with the Sap metalloprotease of *C. crescentus* (21).

144 The S-layer protein (H8GFV3) of *M. album* BG8 is 4,036 amino acids long and
145 contains a conserved hemolysin-type (RTX) calcium-binding region (IPR018511) (17) and
146 a CalX-like domain (IPR038081), with only 35% amino acid identity to the S-layer protein
147 identified in *M. buryatense* 5GB1 (Fig. 3). S-layer proteins are known to display broad
148 diversity between species (22) and the amino acid identity observed between the
149 sequences of S-layer proteins from *M. album* BG8 and *M. buryatense* 5GB1 is above the
150 typical threshold required to consider shared functions (23). In addition, similarly to what
151 is found in *M. album* BG8, a Ca^{+} binding domain was also identified in the RsaA S-layer
152 protein of *C. crescentus* (14). Other Gammaproteobacteria that encode homologues to the
153 H8GFV3 S-layer protein include the close relative, *Methylomicrobium lacus* (49% AA ID)
154 and several strains of *Marinobacterium georgiense* (36-37% AA ID)(Supp. Table 3) for

155 which S-layers and membrane blebs have been reported (24). The S-layer proteins of *M.*
156 *album* BG8, *M. buryatense* 5GB1 and *M. alcaliphilum* 20Z are encoded in gene clusters along
157 with T1SS proteins (H8GF0, H8GF1, H8GF2) (25), which is further evidence of co-
158 regulation and concerted activity of S-layers and the T1SS.

159 The copper regulated CorA and CorB proteins of *M. album* BG8 possess Ca^{2+} binding
160 channels (12, 26), and in conjunction with the TonB-ExbB-ExbD transporter system, they
161 can mediate copper and divalent cation uptake and ion homeostasis (26). Correspondingly,
162 two of the most abundant proteins in the S-layer unit proteome were the TonB siderophore
163 receptor protein (H8GGW0) and a Ca^{2+} binding protein (H8GKK7). However, CorA was only
164 found at low abundance in one proteome replicate (Supp. Table 1). As CorA is considered
165 the anchor for S-layer proteins (8), perhaps it did not remain associated with the released
166 S-layer protein unit, but rather stayed attached to the cell wall, whereas TonB and Ca^{2+}
167 binding proteins remained associated with the S-layer proteins. This could result from a
168 mutation in the *M. album* BG8 *cor*A gene leading to the unit-releasing phenotype, similar to
169 what was observed for *M. alkaliphilum* 20Z (8), but sequence analysis of the *M. album* BG8
170 *corA* gene showed no mutations (data not shown). Furthermore, as neither copper
171 starvation nor growth in 50X trace element solution changed the pattern of S-layer
172 production and release in *M. album* BG8, this phenotype does not appear to be regulated by
173 the abundance of trace metals. Aside from CorA, the highly expressed LPS assembly protein
174 may play a role in linking the S-layer to the cell wall in a calcium-dependent fashion similar
175 to the S-layer of *C. crescentus* (27). But without CorA, the LPS assembly protein may not be
176 sufficient to keep S-layer proteins from being released.

177 Although S-layers seem to be fairly common among methanotrophic bacteria, *M.*
178 *album* BG8 was the only methanotroph out of 8 examined from both Alpha- and
179 Gammaproteobacteria to prolifically release its S-layer units. Structures in TEM images
180 surrounding the methanotrophs other than *M. album* BG8 included white patches from the
181 phosphotungistic acid negative stain (Fig. 2), membrane protrusions around the surface of
182 *M. oleiharenae* XLMV4^{T} cells (Fig. 2e) (28), sparse spherical particles around some *M.*
183 *buryatense* 5GB1 cells (Fig. 2f), and capsule layer surrounding *M. capsulatus* Bath (Fig. 2g)
184 (29) .

185 **Application of the T1SS and released S-layer proteins for bioindustrial protein**
186 **production.** The industrialization of methanotrophs has been growing in appeal due to the
187 potential to convert methane, a potent greenhouse gas and cheap feedstock, into value-
188 added products such as small metabolites, biofuel precursors, biopolymers, and proteins
189 (30). The so far unique phenotype of *M. album* BG8 observed here, wherein S-layer units
190 are delivered from the cytoplasm to the cell surface by the T1SS (31) and then released to
191 the external environment, represents an advantageous protein-production platform. Using
192 the S-layer system, different strategies can be targeted: a heterologous protein can be fused
193 to residues used for excretion through the T1SS for expression of single protein molecules,
194 or the protein of interest can be fused to the N-terminal of the S-layer protein (32) to
195 produce functionalized S-layer units within the culture medium. Of course, the success of
196 such strategies is dependent on the structure and function of the protein of interest but, in
197 each case, the recovery of a heterologous product may be facilitated by the excretion and
198 release mechanism of S-layer units, greatly simplifying downstream processing and
199 reducing associated costs.

200 **Conclusion.** This study identified and characterized a unique phenotype of *M.*
201 *album* BG8 among 8 screened methanotrophic strains. The prolific production and release
202 of *M. album* BG8 S-layer units into the culture medium allowed for their purification and
203 proteomic analysis. We identified a role of the T1SS in S-layer biogenesis and the
204 association of metal-acquisition and membrane biogenesis proteins alongside S-layer
205 protein units. The energy required to produce and release S-layer units is likely
206 considerable, yet *M. album* BG8 grows efficiently and rapidly on both methane and
207 methanol, with a relatively high growth rate compared to other methanotrophs (3). The S-
208 layer production and release phenotype of *M. album* BG8 presents an opportunity to
209 produce and secrete products of bioindustrial interest from the use of single-carbon
210 feedstocks.
211

212 **Materials and Methods**

213 **Culturing conditions and media**. Eight methanotroph strains maintained in the
214 Stein laboratory were used: Gammaproteobacteria - *Methylomicrobium album* BG8,
215 *Methylomonas denitrificans* FJG1, *Methylicorpusculum oleiharenae* XLMV4T, *Methylococcus*
216 *capsulatus* Bath and *Methylotuvimicrobium buryatense* 5GB1; Alphaproteobacteria -
217 *Methylocystis* sp. WRRC1, *Methylocystis* sp. Rockwell, and *Methylosinus trichosporium* OB3b.
218 Methanotrophs were cultivated in 250-mL Wheaton bottles fitted with screw cap lids inlaid
219 with a butyl rubber septum filled with 100 mL of nitrate (NMS) or ammonium mineral salts
220 (AMS) medium (3), or NMS2 medium (33) for *M. buryatense* 5GB1. Gas headspace (50 mL)
221 was removed from each bottle after which methane (60 mL) was injected via syringe fitted
222 with a 0.22-μm filter. For *M. album* BG8 grown on methanol, 100 μL of high-performance

223 liquid chromatography grade methanol (Sigma-Aldrich) was added. Experiments with
224 increased trace metals included 50X standard trace element solution. Experiments with
225 copper-free media included Chelex 100 (BioRad)-treated media (except the trace-elements
226 solution) added to acid-washed Wheaton bottles. 1 mL (1%) inoculum from a late
227 exponential phase culture that had been passaged at least once under the identical growth
228 conditions for each experimental condition was used for each strain. Cultures were
229 incubated at 30°C, with the exception of 37°C for *M. capsulatus* Bath, with shaking at 150
230 rpm until early stationary phase as determined by growth curves (OD_{540}) (3).

231 **Transmission electron microscopy imaging**. Cells (ca. 2 mL) were removed from
232 cultures and pelleted by centrifugation (5 min at 6000 x *g*; Eppendorf). Cell pellets were
233 rinsed and resuspended in 500 µL phosphate buffer. Cell samples were placed on a 300-nm
234 copper grid for 4 to 6 min prior to staining with 1% phosphotungistic acid. Images were
235 captured using a Philips/FEI Transmission Electron Microscope with Gatan Camera
236 (Morgagni). Fig. 2 was imaged with a JEOL JEM-ARM200CF S/TEM electron microscope at
237 an accelerating voltage of 200 kV. The HAADF-STEM images were collected with the JEOL
238 HAADF detector using the following experimental conditions: probe size 6C, condenser
239 lens aperture 30 µm, scan speed 32 µs per pixel, and camera length 8 cm. The average
240 diameter of S-layer proteins starting from the outer edge were measured using ImageJ
241 (n=50).

242 **S-layer purification.** Three technical replicates were used for purification and LC
243 MS/MS proteomics with each replicate deriving from 1 L of *M. album* BG8 culture grown in
244 NMS medium with methane. The purification method is illustrated in Fig. 4, and was
245 adapted from a protocol for isolation of outer membrane vesicles (34). For each replicate,

246 the cultures were filtered using a 0.45-μm PES stericup (Millipore) to separate biomass
247 from filtrate containing the S-layer proteins. The filtrate was passed through a 100 kDa MW
248 cutoff protein concentrator (GE Vivaspin) and retentate was collected by rinsing the filter
249 with 1 mL phosphate buffer at pH 6.8. Retentate aliquots were spotted on NMS agar and
250 incubated with methane to confirm the absence of viable *M. album* BG8 cells.

251 The crude retentate was mixed with OptiPrep (iodixanol; Sigma-Aldrich) (60%) and
252 placed at the bottom of a sterile centrifuge tube. A discontinuous density gradient was
253 created by layering 2 mL of diluted OptiPrep (40, 35, 30, 25, 20% using OptiPrep Diluent)
254 as per manufacturer's instructions. Samples were centrifuged for 12 h at 53,000 rpm
255 (~288,350 x *g*) at 4°C in a Ti70 Fixed rotor ultracentrifuge (Beckman Optima L-90K
256 Ultracentrifuge). 1-mL fractions were removed by pipetting from the top of the density
257 gradient, with a total of 18 fractions per replicate. Each fraction was measured for
258 refractive index (Reichert AR200 Automatic Digital Refractometer) to ensure that the
259 density gradient was maintained. Per fraction, 50 μL was denatured using 50 μL of 2x
260 Laemmli Sample Buffer (BioRad) and incubation on a heat block (Baxter Canlab H2025-1
261 Dry Block Heater) at 95°C for 5 min. The prepared samples were separated on an 8%
262 acrylamide gel and stained with colloidal Coomassie to determine protein presence.
263 Protein-containing fractions were denatured and concentrated using a protein centrifuge
264 concentrator (Amicon) to a final volume of 50 μL. Concentrated protein samples were
265 partially resolved through a precast 4-20% acrylamide gradient gel (BioRad) to remove the
266 Optiprep solvent until no residual sample was present in the wells of the gel. Protein
267 samples were excised from the gel and submitted for LC-MS/MS analysis.

268 **In-Gel Digest of S-layer Peptides.** The gel bands were cut into small pieces and
269 destained four times with 50% Acetonitrile (ACN; Sigma) in 50 mM trietylammonium
270 bicarbonate (TEAB; Sigma) at 37°C for 10 min. Destained gel pieces were washed with 100
271 mM TEAB at 37°C for 10 min and dehydrated by incubating them twice in 100 % ACN at
272 room temperature for 10 min to complete drying. Cysteine residues were reduced by
273 incubating dried gel slices in 10 mM dithiothreitol (DTT; BioRad) solution in 100 mM TEAB
274 for 45 min at 37°C. Reduction solution was replaced with 55 mM iodoacetamide (IA; Sigma)
275 in 100 mM TEAB buffer and incubated in the dark for 1 h at 37°C to alkylate cysteine
276 residues. The alkylation solution was replaced by 100 mM TEAB and incubated for 10 min,
277 repeated twice. Gel pieces were then dehydrated once more in 100% ACN and dried as
278 stated above. Gel pieces were rehydrated by adding 6 ng/μL trypsin (Promega; V5113) in
279 100 mM TEAB. Peptides were digested for 16 h at 37 °C with shaking at 150 rpm. Tryptic
280 peptides were retained, and in-gel digested peptides were further extracted by incubating
281 in 1% (v/v) formic acid (FA; Fisher), 2% (v/v) ACN in 100 mM TEAB for 1 h at 37°C. This
282 was followed by a second 1 h 37°C extraction using a 1:1 1% (v/v) FA in 100 mM TEAB and
283 100% ACN extraction buffer. Digested peptide fractions were pooled and dried. Isolated
284 peptides were re-suspended and desalted using ZipTip C18 pipette tips (ZTC18S960;
285 Millipore), as described (35). All peptides were dried and re-suspended in 3% (v/v) ACN /
286 0.1% (v/v) FA immediately prior to mass spectrometry analysis.
287 **Liquid chromatography mass spectrometry.** Re-suspended tryptic peptides were
288 analyzed using nano flow HPLC (Easy-nLC 1000, Thermo Scientific) with an EASY-Spray
289 capillary HPLC column (PepMap RSLC C18, 75um x 25cm, 100Å, 2μm, Thermo Scientific)
290 coupled to a Q Exactive Orbitrap mass spectrometer (Thermo Scientific). Dissolved samples

291 were injected using an Easy-nLC 1000 system (Thermo Scientific). The column was
292 equilibrated with 100% solvent A (0.1% (v/v) FA, 4% (v/v) ACN in water). Peptides were
293 eluted using the following gradient of solvent B (0.1% (v/v) FA in 80% (v/v) ACN): 0–18%
294 B, 0–73 min; 18–30% B, 73-101 min; 30–46% B, 101–120 min; 46–100% B, 120-123, min
295 at a flow rate of 0.35 µl min−1 at 50°C. High-accuracy mass spectra were acquired in data-
296 dependent acquisition mode. All precursor signals were recorded in a mass range of 300–
297 1,700 m/z and a resolution of 35,000 at 200 m/z. The maximum accumulation time for a
298 target value of 1×10^6 was set to 120 ms. Up to 12 data-dependent MS/MS were recorded
299 using quadrupole isolation with a window of 2 Da and higher-energy collisional
300 dissociation fragmentation with 26% fragmentation energy. A target value of 5×10^4 was
301 set for MS/MS using a maximum injection time of 250 ms and a resolution of 17,500 at 200
302 m/z. Precursor signals were selected for fragmentation with charge states from +2 to +7
303 and a signal intensity of at least 1×10^4. All precursor signals selected for MS/MS were
304 dynamically excluded for 30s.

305 All acquired mass spectrometry data was analyzed using Proteome Discoverer (ver.
306 2.4.1.15). Data were searched against the *M. album* BG8 proteome (UNIPROT
307 H8GRI8_METAL; containing 3,738 protein sequences) using an automatically generated
308 decoy database and the Proteome Discoverer processing workflow
309 (PWF_QE_Basic_SeaquestHT) and consensus workflow (CWF_Basic) with minimal
310 deviation. Deviations included: a precursor and fragment mass tolerance of 10 ppm and 0.6
311 da, respectively, trypsin digestion with 2 missed cleavages, variable modifications
312 methionine oxidation (+15.995 Da), n-terminal acetylation (+42.011 Da), methionine loss (-

313 131.040 Da), methionine loss + n-terminal acetylation (-89.030 Da) and fixed modifications
314 carbamidomethylation (+57.021 Da).

315 **Identifying similar protein sequences in other methanotrophs.** To determine if
316 identified S-layer associated proteins were unique to *M. album* BG8, each identified protein
317 sequence was compared using BLASTp to the gammaproteobacterial methanotrophs:
318 *Methylomonas denitrificans* FJG1 (taxon:416); *Methylicorpusculum oleiharenae* XLMV4T
319 (taxon:1338687); *Methylotuvimicrobium buryatense* 5GB1 (taxon:1338687); and
320 *Methylococcus capsulatus* Bath (taxon:414). (https://blast.ncbi.nlm.nih.gov/). The presence
321 of T1SS proteins identified in the *M. album* BG8 genome (GenBank: CM001475.1) were also
322 analyzed for their presence in the above gammaproteobacterial genomes. For query
323 sequences with a high number of BLASTp hits, only matches with the highest percent
324 identities to the query were reported.

325 To determine the presence of S-layer related proteins in gammaproteobacterial
326 methanotrophs that were not analyzed in this experiment, the proteins of interest were
327 screened against the entire *Methylococcaceae* group (taxid:135618) using BLASTp
328 (Supplemental Table 2). The S-layer protein H8GFV3 was further screened via BLASTp
329 against all Gammaproteobacteria (taxid:1236) (Supplemental Table 3).

330

331 **Acknowledgments:** The authors would like to thank Arlene Oatway and Dr. Kacie Norton
332 from the Biological Sciences Microscopy Unit and Haoyang Yu from NanoFAB with assisting
333 in transmission electron microscopy imaging. All peptide digestion and LC-MS/MS
334 preparation were performed at the Alberta Proteomics and Mass Spectrometry Facility at
335 the Univ. Alberta.

336

337 **Data availability**: All raw proteomics files were submitted to the PRoteomics

338 IDEntification Database (PRIDE; https://www.ebi.ac.uk/pride/). Reviewer access details

339 are as follows: Dataset: PXD050176, Username: reviewer_pxd050176@ebi.ac.uk,

340 Password: pGJMeScS

341

342 **Funding statement**: This work was supported by NSERC Discovery grants to LYS and DS,

343 Canada First Research Excellence Funds (Future Energy Systems) awarded to DS and LYS,

344 and CFI John Evans Leadership Fund (JELF) funding provided to RGU.

345

346 **Conflict of interest**: the authors have no conflicts of interest to declare.

347

348 **Author Contributions**: **Author Contributions:** M.K.H., D.S. and L.Y.S. conceptualized the

349 research. M.K.H. carried out the experiments and created the figures and tables. R.G.U. and

350 M.C.R.G. provided peptide digestion, LC-MS/MS preparation and corresponding proteome

351 analysis. A.M.G. provided bioinformatics analysis. M.K.H. and L.Y.S. wrote the manuscript.

352 D.S and L.Y.S edited the manuscript and supervised the work. All authors have given

353 consent to the final version of the manuscript.

354

355 **Permission to print information from another source**. Figure 1 was an adapted

356 protocol with permission from Microbiological Research.

357

Originality statement: None of the work in this manuscript has been published or submitted for publication elsewhere.

References:

1. Khmelenina VN, But SY, Rozova ON, Trotsenko YA. 2019. Metabolic features of aerobic methanotrophs: news and views. Curr Issues Mol Biol 33:85-99.
2. Kang NK, Chau THT, Lee EY. 2024. Engineered methane biocatalysis: strategies to assimilate methane for chemical production. Curr Op Biotechnol 85:103031.
3. Tays C, Guarnieri MT, Sauvageau D, Stein LY. 2018. Combined effects of carbon and nitrogen source to optimize growth of proteobacterial methanotrophs. Front Microbiol 9:2239.
4. Sugden S, Lazic M, Sauvageau D, Stein LY. 2021. Transcriptomic and metabolomic responses to carbon and nitrogen sources in *Methylomicrobium album* BG8. Appl Environ Microbiol 87.
5. Villada JC, Duran MF, Lim CK, Stein LY, Lee PKH. 2022. Integrative genome-scale metabolic modeling reveals versatile metabolic strategies for methane itilization in *Methylomicrobium album* BG8. mSystems 7:e0007322.
6. Khmelenina VN, Suzina NE, Trotsenko YA. 2013. Surface layers of methanotrophic bacteria. Microbiology 82:529-541.
7. Trotsenko YA, Khmelenina VN. 2002. The biology and osmoadaptation of haloalkaliphilie methanotrophs. Microbiology 71:123-132.
8. Shchukin VN, Khmelenina VN, Eshinimayev BT, Suzina NE, Trotsenko YA. 2011. Primary characterization of dominant cell surface proteins of halotolerant methanotroph *Methylomicrobium alcaliphilum* 20Z. Microbiology 80:608-618.
9. Khmelenina VN, Shchukin VN, Reshetnikov AS, Mustakhimov, II, Suzina NE, Eshinimaev BT, Trotsenko YA. 2010. Structural and functional features of methanotrophs from hypersaline and alkaline lakes. Microbiology 79:472-482.
10. Jeffries P, Wilkinson JF. 1978. Electron microscopy of cell wall complex of *Methylomonas albus*. Arch Microbiol 119:227-229.
11. Kim HG, Han GH, Eom CY, Kim SW. 2008. Isolation and taxonomic characterization of a novel type I methanotrophic bacterium. J Microbiol 46:45-50.
12. Johnson KA VT, Larsen Ø, Pedersen RB, Lillehaug JR, Jensen HB, et al. 2014. CorA is a copper repressible surface-associated copper(I)-binding protein produced in *Methylomicrobium album* BG8. Plos One 9:e87750.
13. Berson O, Lidstrom ME. 1997. Cloning and characterization of *corA*, a gene encoding a copper-repressible polypeptide in the type I methanotroph, *Methylomicrobium albus* BG8. FEMS MIcrobiol Lett 148:169-174.
14. Bharat T, Kureisaite-Ciziene, D., Hardy, G. et al. 2017. Structure of the hexagonal surface layer on Caulobacter crescentus cells. Nat Microbiol 2:17059.
15. Herrmann J, Jabbarpour F, Bargar PG, Nomellini JF, Li PN, Lane TJ, Weiss TM, Smit J, Shapiro L, Wakatsuki S. 2017. Environmental calcium controls alternate physical states of the *Caulobacter* surface layer. Biophys J 112:1841-1851.
16. Bao K, Claesson R, Gehrig P, Grossmann J, Oscarsson J, Belibasakis GN. 2022. Proteomic characterization of the oral pathogen *Filifactor alocis* reveals key inter-protein pnteractions of Its RTX toxin: FtxA. Pathogens 11.
17. Linhartová I, Bumba L, Mašín J, Basler M, Osička R, Kamanová J, Procházková K, Adkins I, Hejnová-Holubová J, Sadílková L, Morová J, Sebo P. 2010. RTX proteins: a highly diverse family secreted by a common mechanism. FEMS Microbiol Rev 34:1076-112.

18. Bumba L, Masin J, Macek P, al. e. 2016. Calcium-Driven Folding of RTX Domain β-Rolls Ratchets Translocation of RTX Proteins through Type I Secretion Ducts. Molec Cell 62:47-62.
19. Samsudin F, Ortiz-Suarez ML, Piggot TJ, Bond PJ, Khalid S. 2016. OmpA: A Flexible Clamp for Bacterial Cell Wall Attachment. Structure 24:2227-2235.
20. Spitz O, Erenburg IN, Beer T, Kanonenberg K, Holland IB, Schmitt L. 2019. Type I secretion systems-one mechanism for all? Microbiol Spect 7:10.1128/microbiolspec.psib-0003-2018.
21. Ford MJ, Nomellini JF, Smit J. 2007. S-Layer anchoring and localization of an S-Layer-associated protease in *Caulobacter crescentus*. J Bacteriol 189:2226-2237.
22. Fagan R, Fairweather N. 2014. Biogenesis and functions of bacterial S-layers. Nat Microbiol 12:211-222.
23. Sander C, Schneider R. 1991. Database of homology-derived protein structures and the structural meaning of sequence alignment. Proteins 9:56-68.
24. González JM, Mayer F, Moran MA, Hodson RE, Whitman WB. 1997. Microbulbifer hydrolyticus gen. nov., sp. nov., and Marinobacterium georgiense gen. nov., sp. nov., Two Marine Bacteria from a Lignin-Rich Pulp Mill Waste Enrichment Community. Int J Syst Evol Microbiol 47:369-376.
25. Hamilton R, Gebbie W, Bowman C, Mantanona A, Kalyuzhnaya MG. 2024. Microbial Hauberks: Composition and Function of Surface Layer Proteins in Gammaproteobacterial Methanotrophs. bioRxiv doi:https://doi.org/10.1101/2024.07.09.602694
26. Khmelenina VN, Suzina NE, Trotsenko YA. 2013. Surface layers of methanotrophic bacteria. Microbiology 82:529–541.
27. von Kügelgen A, Tang H, Hardy GG, Kureisaite-Ciziene D, Brun YV, Stansfeld PJ, Robinson CV, Bharat TAM. 2020. In situ structure of an intact lipopolysaccharide-bound bacterial surface layer. Cell 180:348-358.e15.
28. Saidi-Mehrabad A, Kits DK, Kim JJ, Tamas I, Schumann P, Khadka R, Strilets T, Smirnova AV, Rijpstra WIC, Damsté JSS, Dunfield PF. 2020. *Methylicorpusculum oleiharenae* gen. nov., sp. nov., an aerobic methanotroph isolated from an oil sands tailings pond. Int J Syst Evol Microbiol 70:2499-2508.
29. Whittenbury R, Phillips KC, Wilkinson JF. 1970. Enrichment, isolation and some properties of methane-utilizing bacteria. J Gen Microbiol 61:205-218.
30. Pham DN, Nguyen AD, Lee EY. 2022. Outlook on engineering methylotrophs for one-carbon-based industrial biotechnology. Chem Eng J 449.
31. Kalyuzhnaya M, Demidenko O, Collins D. 2018. Compositions and methods using methanotrophic s-layer proteins for expression of heterologous proteins. USA.
32. Sára M, Sleytr UB. 2000. S-Layer Proteins. J Bacteriol 182:859-868.
33. Puri AW, Owen S, Chu F, Chavkin T, Beck DAC, Kalyuzhnaya MG, Lidstrom ME. 2015. Genetic tools for the industrially promising methanotroph *Methylomicrobium buryatense*. Appl Environ Microbiol 81:1775-1781.
34. Klimentová J, Stulík J. 2015. Methods of isolation and purification of outer membrane vesicles from gram-negative bacteria. MIcrobiol Res 170:1-9.
35. Uhrig RG, Schläpfer P, Roschitzki B, Hirsch-Hoffmann M, Gruissem W. 2019. Diurnal changes in concerted plant protein phosphorylation and acetylation in Arabidopsis organs and seedlings. Plant J 99:176-194.

446 **Table 1**. Average diameter of *M. album* BG8 S-layer protein units (n=50) per tested media

447 condition.

Media Condition	Avg. Size (nm)	Range (nm)
CH_4/NMS	60.9 ± 5.7	49.5 – 75.2
CH_4/AMS	64.5 ± 6.5	49.2 – 78.7
CH_3OH/NMS	64.8 ± 8.1	49.7 – 84.0
CH_3OH/AMS	66.9 ± 4.8	54.4 – 77.5
CH_4/x50 trace elements	61.0 ± 6.8	53.1 – 78.0
CH_4/vitamin stock	67.0 ± 6.7	49.4 – 82.0

448

449

450 **Table 2.** Significant peptide hits from LC-MS/MS detection of purified released S-layer

451 protein units (n=3).

Accession	UniProt Description	Mean PSM	Mean peptide	Mean score	COG Category
H8GMU5	Flagellin	331.7	22.3	1316.7	Cell motility
H8GHU9	Prepilin-type N-terminal cleavage/methylation domain-containing protein	64.3	4.0	231.4	Intracellular trafficking, secretion, and vesicular transport
H8GNA1	Uncharacterized protein (Metallo-protease PrtC*)	30.3	15.7	106.7	Secondary metabolites biosynthesis, transport and catabolism
H8GIF1	Type I secretion C-terminal target domain protein	24.5+	12.5+	71.9+	Secondary metabolites biosynthesis, transport and catabolism
H8GNF7	Flagellar hook protein FlgE	16.0	8.7	51.7	Cell motility
H8GGQ6	Uncharacterized protein	16.0	4.7	52.5	-
H8GIA0	ATP synthase epsilon chain	9.7	1.0	22.4	Lipid transport and metabolism
H8GJI6	LPS-assembly protein LptD	16.7	2.7	43.8	Cell wall/membrane/envelope biogenesis
H8GJ49	Outer membrane cobalamin receptor protein	8.0	6.3	22.5	Coenzyme transport and metabolism
H8GGW0	TonB-dependent siderophore receptor	7.0	6.3	20.2	Inorganic ion transport and metabolism
H8GKK7	Ca2+-binding protein, RTX toxin	5.7	5.7	18.5	Secondary metabolites biosynthesis, transport and catabolism
H8GKR0	Uncharacterized protein (Outer membrane protein*)	5.0	2.0	17.9	Cell wall/membrane/envelope biogenesis
H8GFV3	S-layer protein	7.3	6.3	23.2	Secondary metabolites biosynthesis, transport and catabolism
H8GPP0	Uncharacterized protein	7.0	1.0	20.0	Inorganic ion transport and metabolism

*HHpred protein annotation (>95% probability)
+ replicates n=2

452
453

454

455 **Table 2**. Additional protein hits of interest from LC-MS/MS detection of purified released

456 S-layer protein units.

Accession	UniProt Accession	Mean PSM	Mean Peptide	Mean Score	COG Category
H8GMU7	Flagellar hook-associated protein 2	5.00	5.00	13.49	Cell motility
H8GL31	Cell division coordinator CpoB	5.00	5.00	11.65	Cell cycle control, cell division, chromosome partitioning
H8GNA4	Uncharacterized protein	4.67	2.00	11.77	-
H8GL29	Tol-Pal system protein TolB	4.67	4.33	14.22	Intracellular trafficking, secretion, and vesicular transport
H8GRD0	Transaldolase	4.33	4.00	10.21	Nucleotide transport and metabolism
H8GN21	Uncharacterized protein	4.00	1.00	8.92	Function unknown
H8GNM8	Hemolysin-coregulated protein (Uncharacterized)	3.67	3.00	10.30	Function unknown
H8GM80	Uncharacterized protein	3.33	1.00	7.05	-
H8GG32	Adenosylhomocysteinase	3.33	1.33	4.80	Coenzyme transport and metabolism
H8GFV2	Type I secretion outer membrane protein, TolC family	3.00	3.00	8.09	Cell wall/membrane/envelope biogenesis; Intracellular trafficking, secretion, and vesicular transport
H8GK80	Outer membrane protein/peptidoglycan-associated (Lipo)protein	3.00	2.33	8.32	Cell wall/membrane/envelope biogenesis
H8GI44	PQQ-dependent dehydrogenase, methanol/ethanol family	3.00	3.00	7.40	Carbohydrate transport and metabolism
H8GQ61	Uncharacterized protein	3.00	2.67	7.27	Function unknown
H8GNG3	Flagellar hook-associated protein 1	2.67	2.67	8.48	Cell motility
H8GPY3	Outer membrane protein/peptidoglycan-associated (Lipo)protein	2.67	2.33	7.49	Cell wall/membrane/envelope biogenesis
H8GGQ9	DNA-binding transcriptional regulator NtrC	2.67	1.00	6.79	Signal transduction mechanisms
H8GGW4	Uncharacterized protein	2.67	1.00	6.78	Function unknown
H8GNG4	Flagellar hook-associated protein 3	2.33	2.33	6.55	Cell motility
H8GI88	Probable cytosol aminopeptidase	2.33	2.00	6.21	Amino acid transport and metabolism
H8GPH9	Uncharacterized protein	1.67	1.67	6.06	Function unknown

H8GI24	Uncharacterized protein	4.00[a]	1.00	10.57	-
H8GI56	Uncharacterized protein	2.50[a]	2.50	6.29	-
H8GH59	PAS domain S-box/diguanylate cyclase (GGDEF) domain-containing protein	3.50[a]	1.00	9.16	Signal transduction mechanisms
H8GK04	Cation diffusion facilitator family transporter	2.50	1.00[b]	6.19	Inorganic ion transport and metabolism
H8GHK8	Gly-zipper_OmpA domain-containing protein	3.50	2.00	12.03[c]	Function unknown
H8GIF2	VCBS repeat-containing protein	2.67	2.00	11.46[c]	Secondary metabolites biosynthesis, transport and catabolism
H8GPX1	Citrate lyase beta subunit	2.33	1.00	8.01[c]	Carbohydrate transport and metabolism
H8GIF8		3.00	2.50	7.94[c]	Cell motility; Intracellular trafficking, secretion, and vesicular transport

[*] HHpred protein annotation (>95%)
[a] Absent in replicate A
[b] Absent in replicate B
[c] Absent in replicate C

Figure Legends:

Figure 1. Transmission electron micrographs of *M. album* BG8 with released S-layer protein units (as depicted with arrows) when cultured with methane in various media conditions. (a) NMS media (b) AMS media without copper (c) NMS media with 50X trace elements solution. Micrographs contain a wide ranges of scales to highlight membrane morphology and adjacent surrounding areas.

Figure 2. Transmission electron micrographs of selected alpha- and gammaproteobacterial methanotrophs cultivated on methane and NMS. (a) *Methylocystis* sp. WRRC1 (b) *Methylocystis* sp. Rockwell (c) *Methylosinus trichosporium* OB3b (d) *Methylomonas denitrificans* FJG1 (e) *Methylicorpusculum oleiharenae* XLMV4^{T} (f) *Methylotuvimicrobium buryatense* 5GB1 (g) *Methylococcus capsulatus* Bath.

Figure 3. Protein sequence comparison of S-layer and T1SS- related proteins of *M. album* BG8 to gammaproteobacterial methanotrophs *M. denitrificans* FJG1, *M. oleiharenae* XLMV4^{T}, *M. buryatense* 5GB1 and *M. capsulatus* Bath.

Figure 4. S-layer isolation and purification protocol for *M. album* BG8 adapted from (34).

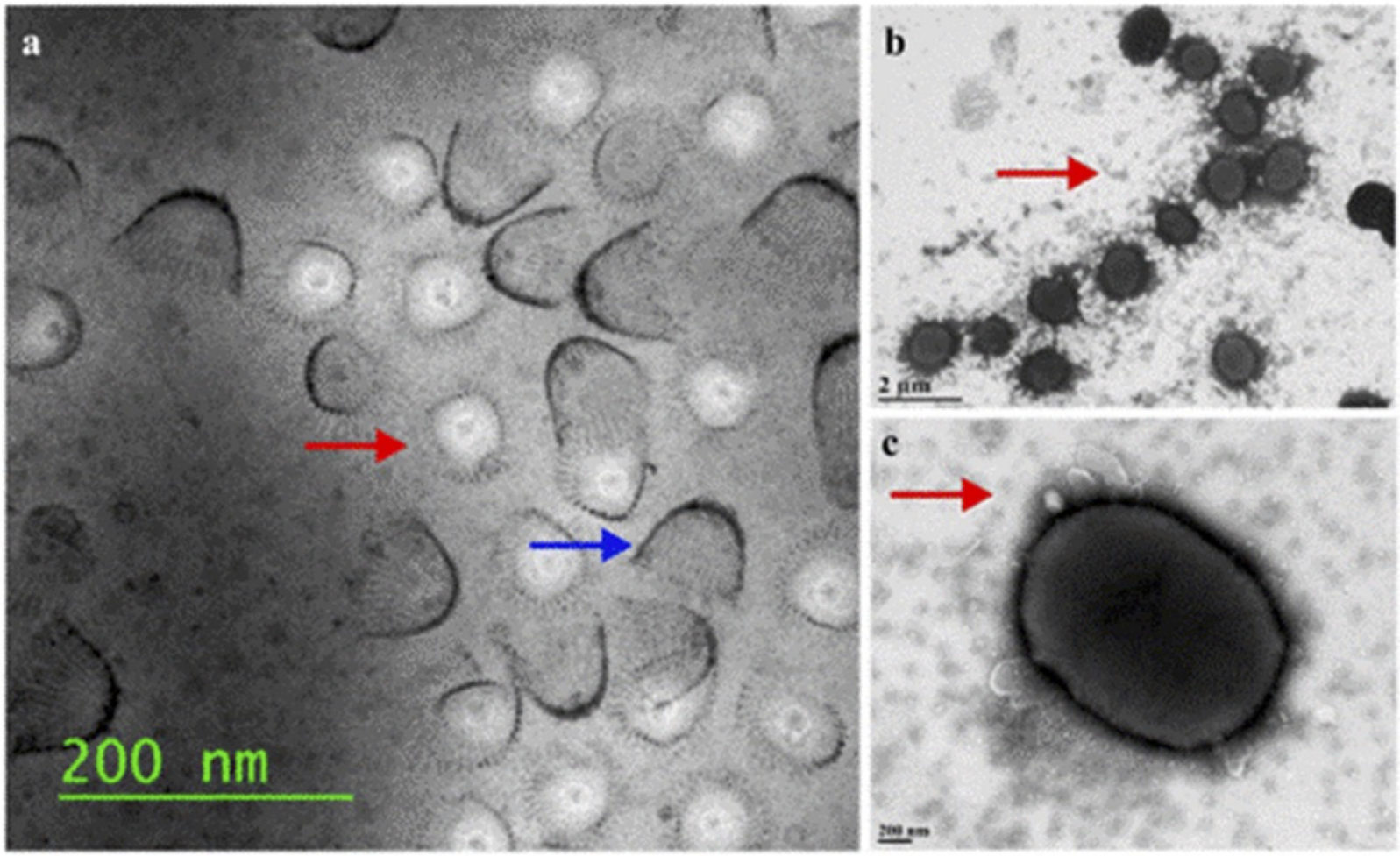
a
200 nm
b
2 µm
c

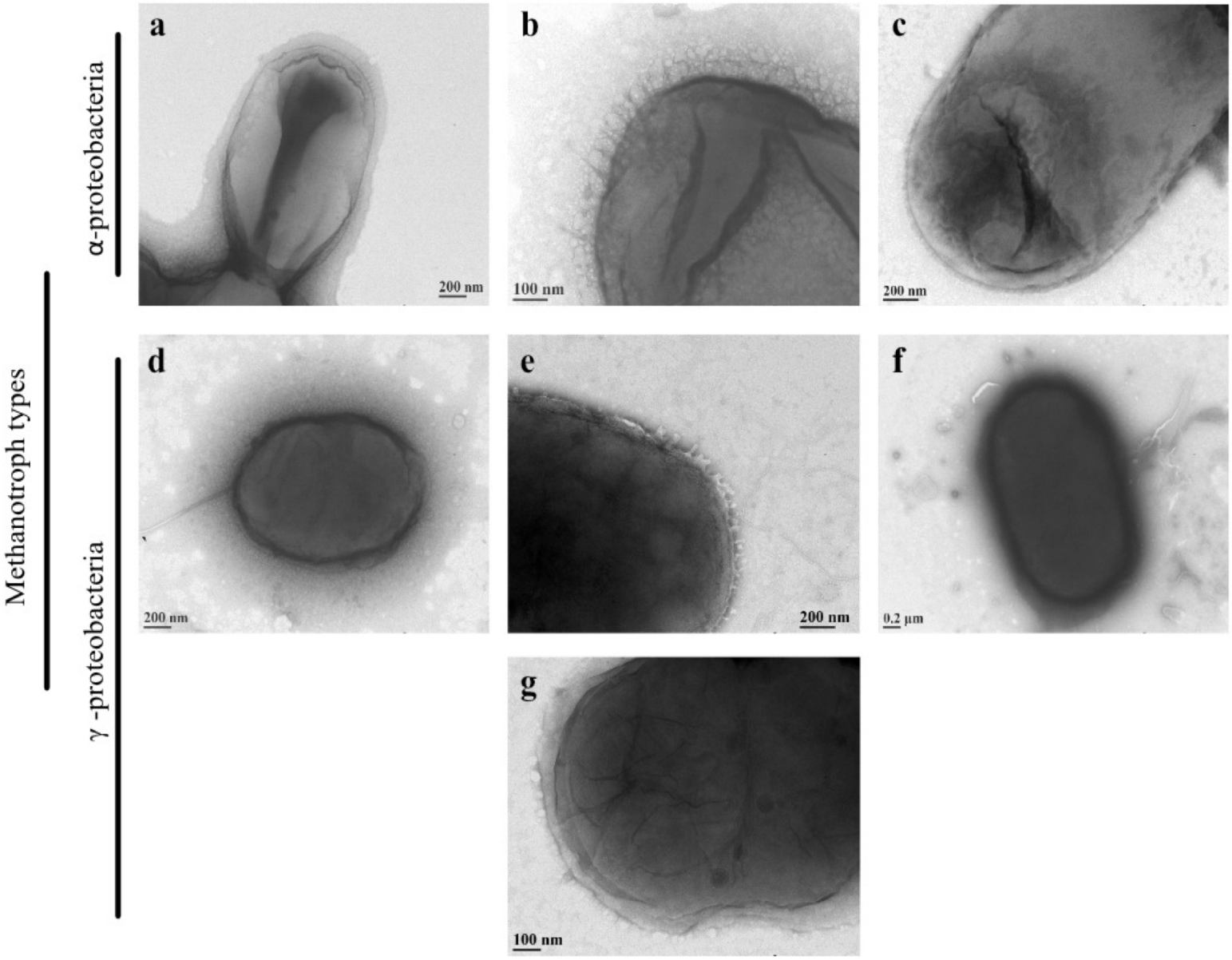
Methanotroph types
α-proteobacteria
γ -proteobacteria
a
200 nm
b
100 nm
c
200 nm
d
200 nm
e
200 nm
f
0,2 µm
g
100 nm

Methylomicrobium album BG8 (taxon:686340)				*Methylomonas denitrificans* FJG1 (taxon:416)				*Methylicorpusculum oleiharenae* XLMV4^{T} (taxon:1338687)				*Methylotuvimicrobium buryatense* 5GB1 (taxon:1338687				*Methylococcus capsulatus* Bath (taxon:414)			
GeneBank ID	Accession	Description	Length (aa)	Reference Sequence	Query Cov	E value	% Identity	Reference Sequence	Query Cov	E value	% Identity	Reference Sequence	Query Cov	E value	% Identity	Reference Sequence	Query Cov	E value	% Identity
EIC29550.1	H8GNF7	Flagellar hook protein FlgE	431	WP_036275189	100%	1.0E-144	52%	WP_159659411.1	100%	9.0E-137	51%	WP_017842460.1	100%	1.0E-135	50%	-	-	-	-
EIC29497.1	H8GMU5	Flagellin	761	WP_036276946.1	31%	1.0E-44	61%	WP_231089167.1	13%	4.0E-24	51%	QCW83869.1	33%	6.0E-48	67%	-	-	-	-
EIC28933.1	H8GHU9	Prepilin-type N-terminal cleavage/methylation domain-containing protein	158	-	-	-	-	-	-	-	-	-	-	-	-	-	-	-	-
EIC28015.1	H8GKK7	Ca2+-binding protein, RTX toxin	1044	AMK76855.1	23%	1.0E-08	29%	WP_159658860.1	27%	3.0E-10	39%	WP_017842713.1	89%	0.0E+00	47%	-	-	-	-
EIC31463.1	H8GIF1	Type 1 secretion C-terminal target domain protein	1392	AMK76855.1	7%	3.0E-12	55%	WP_159658860.1	17%	1.0E-14	55%	WP_175421712.1	14%	3.0E-12	40%	-	-	-	-
EIC29232.1	H8GKR0	Uncharacterized protein	299	WP_036278985.1	91%	4.0E-68	42%	WP_159657453.1	86%	2.0E-70	47%	WP_017840936.1	87%	2.0E-80	46%	WP_010960992.1	87%	2.0E-39	31%
EIC28502.1	H8GPP0	Uncharacterized protein	118	WP_036273854.1	92%	4.0E-57	76%	WP_159658499.1	92%	8.0E-46	62%	-	-			-	-		
EIC31556.1	H8GJ49	Outer membrane cobalamin receptor protein	691	WP_052142199.1	22%	7.0E-07	25%	WP_159657167.1	26%	3.0E-13	27%	WP_017840490.1	21%	5.0E-08	24%	-	-	-	-
EIC30073.1	H8GGW0	TonB-dependent siderophore receptor	787	AMK76721.1	94%	2.0E-65	30%	WP_159658092.1	100%	0.0E+00	73%	WP_017841134.1	92%	3.0E-63	28%	AAU92033.1	22%	2.0E-14	29%
EIC31412.1	H8GIA0	ATP synthase epsilon chain	140	WP_033156953.1	100%	1.0E-49	80%	WP_159657005.1	100%	2.0E-53	84%	WP_026130213.1	100%	1.0E-53	84%	WP_010959386.1	97%	5.0E-35	67%
EIC30346.1	H8GJI6	LPS-assembly protein LptD	1003	WP_062329806.1	95%	0.0E+00	43%	WP_159657794.1	96%	0.0E+00	45%	WP_017842102.1	96%	0.0E+00	47%	WP_228370330.1	85%	0.0E+00	36%
EIC28704.1	H8GFV3	S-layer protein	4036	-	-	-	-	-	-	-	-	WP_017842715.1	43%	1.0E-36	35%	-	-	-	-
EIC28703.1	H8GFV2	Type I secretion outer membrane protein, TolC family	464	WP_036273387.1	89%	1.0E-47	30%	WP_231089141.1	88%	2.0E-41	28%	WP_138767192.1	94%	0.0E+00	63%	WP_010960559.1	94%	3.0E-32	28%
EIC28702.1	H8GFV1	Type I secretion membrane fusion protein, HlyD family*	440	WP_062329159.1	99%	3.0E-38	28%	-	-	-	-	WP_017842711.1	100%	0.0E+00	70%	-	-	-	-
EIC28701.1	H8GFV0	Type I secretion system ABC transporter, PrtD family*	570	WP_062329155.1	92%	1.0E-61	29%	WP_231089186.1	83%	6.0E-55	29%	WP_017842710.1	97%	0.0E+00	80%	WP_010960270.1	42%	1.0E-35	33%
EIC30282.1	H8GIU2	Type I secretion system ATPase, LssB family*	724	WP_062329155.1	96%	0.0E+00	73%	WP_231089186.1	87%	2.0E-86	32%	WP_017841836.1	96%	0.0E+00	63%	WP_010960270.1	42%	3.0E-49	39%
EIC29875.1	H8GR48	Type I secretion outer membrane protein, TolC family*	469	WP_036273387.1	92%	1.0E-151	53%	WP_231089141.1	92%	2.0E-180	60%	WP_017840392.1	94%	0.0E+00	63%	WP_010960559.1	91%	3.0E-98	44%

*Not explicitly present in S-layer proteome

Query Coverage

0% 100%

Percent Identity

0% 100%

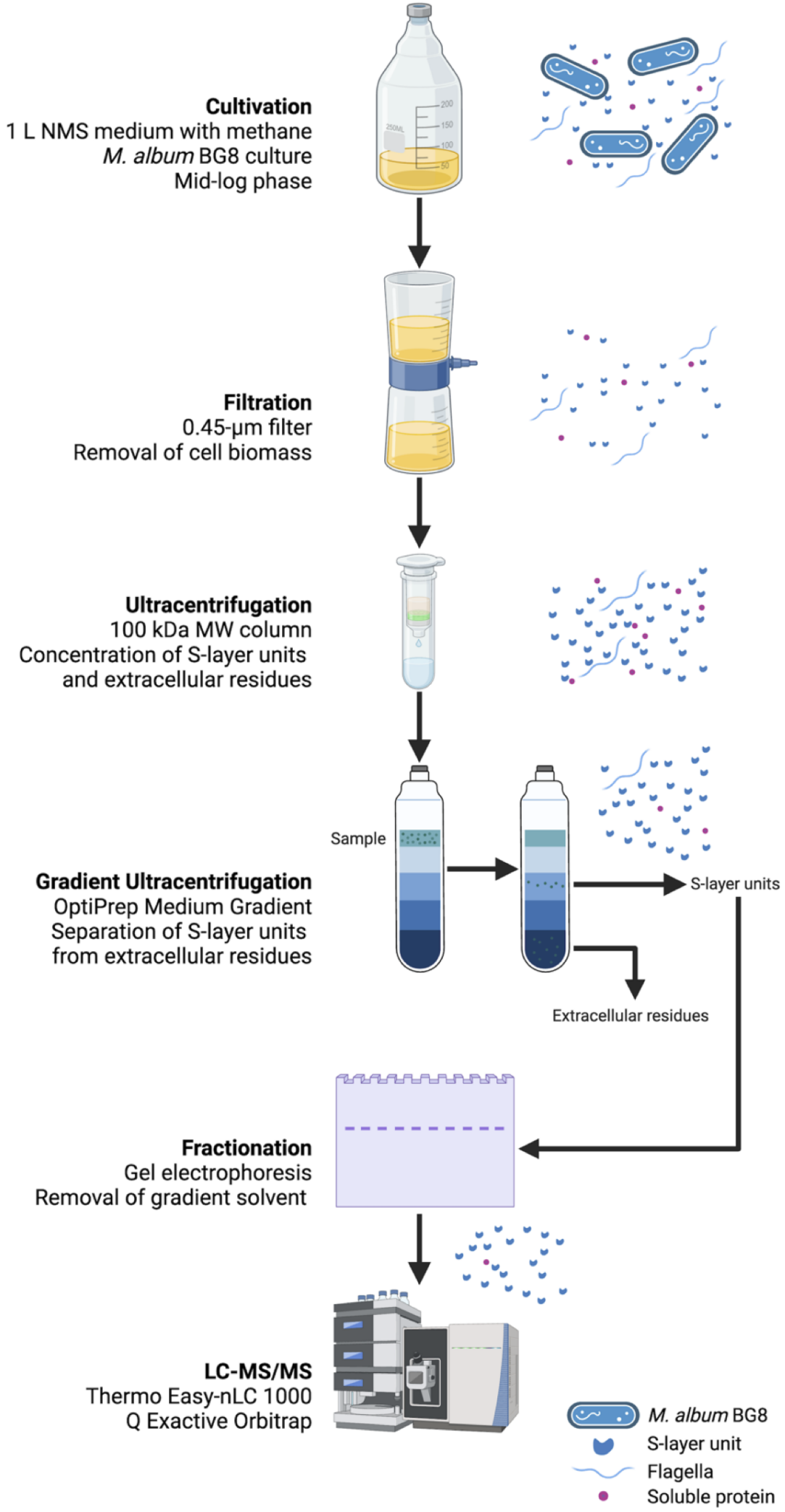
Cultivation
1 L NMS medium with methane
M. album BG8 culture
Mid-log phase
Filtration
0.45-µm filter
Removal of cell biomass
Ultracentrifugation
100 kDa MW column
Concentration of S-layer units
and extracellular residues
Gradient Ultracentrifugation
OptiPrep Medium Gradient
Separation of S-layer units
from extracellular residues
Sample
S-layer units
Extracellular residues
Fractionation
Gel electrophoresis
Removal of gradient solvent
LC-MS/MS
Thermo Easy-nLC 1000
Q Exactive Orbitrap
M. album BG8
S-layer unit
Flagella
Soluble protein